Academic Program [Oral A] | 05. Physical Chemistry -Chemical Kinetics and Dynamics-：Oral A

Tue. Mar 19, 2024 9:00 AM - 11:20 AM JST | Tue. Mar 19, 2024 12:00 AM - 2:20 AM UTC
A1455(1455, Bldg. 14 [5F])

[A1455-2am] 05. Physical Chemistry -Chemical Kinetics and Dynamics-

Chair: Kenichi Okutsu, Toshiaki Nagata

Japanese
9:00 AM - 9:10 AM JST | 12:00 AM - 12:10 AM UTC
[A1455-2am-01]

Collision induced dissociation mass spectrometry of cadmium-sulfide cluster $[Cd_{10}S_4(SPh)_{16}]^{4-}$ and fragment ions

○Keisuke Yukawa[1], Satoru Muramatsu[1], Ryo Takahata[2], Toshiharu Teranishi[2], Yoshiya Inokuchi[1] (1. The Univ. of Hiroshima, 2. The Univ. of Kyoto)

Japanese
9:10 AM - 9:20 AM JST | 12:10 AM - 12:20 AM UTC
[A1455-2am-02]

Structures of silver fluoride cluster cations studied by ion mobility-mass spectrometry

○Yuta Naruse[1], Hiroya Sakakura[2], Yuto Nakajima[2], Keijiro Ohshimo[2], Fuminori Misaizu[2] (1. Faculty of Science, Tohoku University, 2. Graduate School of Science, Tohoku University)

Japanese
9:20 AM - 9:30 AM JST | 12:20 AM - 12:30 AM UTC
[A1455-2am-03]

Ion imaging study on UV-Vis photodissociation processes of O_4^+

○Yu Watabe[1], Takumi Koshiba[2], Yuri Ito[2], Manabu Kanno[2], Keijiro Ohshimo[2], Fuminori Misaizu[2] (1. Faculty of Science, Tohoku Univ. , 2. Graduate School of Science, Tohoku Univ.)

Japanese
9:30 AM - 9:40 AM JST | 12:30 AM - 12:40 AM UTC
[A1455-2am-04]

Study of intramolecular proton transfer reaction mechanisms and their rate constants using cryogenic temperature ion trap-ion mobility mass spectrometry

○Kengo Tsunoda[1], Daiki Fuse[1], Yuya Takasaki[1], Keijiro Ohshimo[1], Fuminori Misaizu[1] (1. Graduate School of Science, Tohoku University)

Japanese
9:40 AM - 9:50 AM JST | 12:40 AM - 12:50 AM UTC
[A1455-2am-05]

Isomer structures of dibenzo-24-crown-8 complex with methylammonium ion studied by cryogenic ion mobility-mass spectrometry

○Kyosuke Watanabe[1], Ryosuke Ito[2], Keijiro Ohshimo[2], Fuminori Misaizu[2] (1. Faculty of Science, Tohoku University, 2. Graduate School of Science, Tohoku University)

English
9:50 AM - 10:00 AM JST | 12:50 AM - 1:00 AM UTC
[A1455-2am-06]

Control of charge state and reactivity of single-sized silver nanoclusters supported on organic substrates

○Takashi Nishikawa[1], Koh Shinomiya[1], Tomoya Inoue[1], Atsushi Nakajima[1] (1. Keio University)

10:00 AM - 10:10 AM JST | 1:00 AM - 1:10 AM UTC

Break

Japanese

10:10 AM - 10:20 AM JST | 1:10 AM - 1:20 AM UTC

[A1455-2am-07]

Generation of multiorder stimulated Raman scattering in CCl_4 droplets studied by temporal profiles

○Ruiji Kataoka[1], Jun-ya Kohno[1] (1. GAKUSHUIN UNIVERSITY)

Japanese

10:20 AM - 10:30 AM JST | 1:20 AM - 1:30 AM UTC

[A1455-2am-08]

Development of gas-phase ion fluorescence spectrometer combined with digital ion trap using droplet-beam IR laser ablation method

○Kenichi Okutsu[1], Takumi Oka[1], Hanako Mizumura[1], Jun-ya Kohno[1] (1. Gakushuin Univ.)

English

10:30 AM - 10:40 AM JST | 1:30 AM - 1:40 AM UTC

[A1455-2am-09]

Dependence of the oscillation of N_2^+ lasing signals at 391 nm on the wavelength of seed laser pulses

○Tomoya Yamauchi[1], Hiroki Mashiko[2], Toshiaki Ando[1], Erik Lötstedt[1], Atushi Iwasaki[1], Kaoru Yamanouchi[1] (1. The Univ. of Tokyo, 2. NTT Advanced Technology Corporation)

English

10:40 AM - 10:50 AM JST | 1:40 AM - 1:50 AM UTC

[A1455-2am-10]

Reactions of iron cationic clusters with hydrogen molecules investigated by gas-phase thermal desorption spectrometry

○Xueshan Wu[1], Yufei Zhang[1], Masato Yamaguchi[1], Toshiaki Nagata[1], Ken Miyajima[1], Fumitaka Mafuné[1] (1. The University of Tokyo)

Japanese

10:50 AM - 11:00 AM JST | 1:50 AM - 2:00 AM UTC

[A1455-2am-11]

Hydrogen storage capacity of rhodium clusters studied by thermal desorption spectrometry in the gas phase

○Hayato Kurashita[1], Yangkun Wu[1], Satoshi Kudoh[1], Masato Yamaguchi[1], Toshiaki Nagata[1], Ken Miyajima[1], Fumitaka Mafuné[1] (1. The Univ. of Tokyo)

English

11:00 AM - 11:10 AM JST | 2:00 AM - 2:10 AM UTC

[A1455-2am-12]

Computational investigation on hydrogen storage capacity of transition metal dimers

○Yufei Zhang[1], Masato Yamaguchi[1], Toshiaki Nagata[1], Satoshi Kudoh[1], Ken Miyajima[1], Fumitaka Mafuné[1] (1. School of Arts and Sciences, The Univ. of Tokyo)

Japanese

11:10 AM - 11:20 AM JST | 2:10 AM - 2:20 AM UTC

[A1455-2am-13]

Photoelectron spectroscopy of precious metal clusters under heating conditions

○Masato Yamaguchi[1], Keitaro Tatsukawa[1], Toshiaki Nagata[1], Ken Miyajima[1], Fumitaka Mafune[1]
(1. The Univ. of Tokyo)

衝突誘起解離質量分析によるカドミウム硫黄クラスター $[Cd_{10}S_4(SPh)_{16}]^{4-}$ および解離イオンの構造評価

（広島大理[1]・広島大院先進[2]・京大化研[3]）○湯川 圭祐[1]・村松 悟[2]・高畑 遼[3]・寺西 利治[3]・井口 佳哉[2]

Collision induced dissociation mass spectrometry of cadmium-sulfide cluster $[Cd_{10}S_4(SPh)_{16}]^{4-}$ and fragments ions

([1]*School of Science, Hiroshima Univ.*, [2]*Grad. School of Advanced Science and Engineering, Hiroshima Univ.* [3] *Institute for Chemical Research, Kyoto Univ.*) ○Keisuke Yukawa[1], Satoru Muramatsu[2], Ryo Takahata[3], Toshiharu Teranishi[3], Yoshiya Inokuchi[2]

We performed collision induced dissociation mass spectrometry (CID-MS) of two cadmium-sulfur clusters $[Cd_9S_4(SPh)_{12}]^{2-}$ (**Cd9**) and $[Cd_9S_4(SPh)_{11}]^{-}$ (**Cd9'**), which were obtained by prompt partial dissociation of $[Cd_{10}S_4(SPh)_{16}]^{4-}$ upon electrospray ionization. It was revealed that the dissociation energy of **Cd9'** is much (by ca. 0.25 eV) larger than **Cd9**. Quantum chemical calculations implied that **Cd9** takes a three-fold symmetric pyramidal structure similar to $[Cd_{10}S_4(SPh)_{16}]^{4-}$, whereas **Cd9'** has rather low-symmetry structure with more Cd–S bonds. We concluded that the above-described large structural difference accounts for the higher durability of **Cd9'** against the collision.

Keywords : Metal cluster; Transition metal chalcogenide; Mass spectrometry; Collision induced dissociation; Quantum chemical calculation

近年，衝突誘起解離質量分析（CID-MS）を配位子保護金属クラスターに適用することで，クラスターコア構造を反映した特異な解離メカニズムが明らかにされてきた(1)。本研究では，正四面体型構造を持つカドミウム硫黄クラスター$[Cd_{10}S_4(SPh)_{16}]^{4-}$(2)にこの手法を適用し，コア構造が解離パターン・解離エネルギーに与える影響を調べることを目的とした。

$[Cd_{10}S_4(SPh)_{16}](NMe_4)_4$／アセトニトリル溶液のエレクトロスプレーイオン化（ESI）質量分析を行うと，対象クラスターの速やかな解離によって生じた Cd 9 量体クラスター$[Cd_9S_4(SPh)_{12}]^{2-}$（**Cd9**）および $[Cd_9S_4(SPh)_{11}]^{-}$（**Cd9'**）が観測された。これらは SPh^- 配位子の数が 1 つだけ異なる。そこで，それぞれを質量選別して CID-MS を試みたところ，解離に要するエネルギーが大きく（約 0.25 eV）異なることが見出された（Fig. 1）。量子化学計算によると，**Cd9** は$[Cd_{10}S_4(SPh)_{16}]^{4-}$の構造を反映した 3 回対称のピラミッド構造をとるのに対し，**Cd9'**は一部の$(Cd–S)_3$ 6 員環ユニットを崩して$(Cd–S)_2$ 4 員環を形成することで低対称ながらより多くの Cd–S 結合数を持つコア構造をとり（Fig. 1），上述の解離エネルギーの違いに寄与することが示唆された。すなわち，本研究により，カドミウム硫黄クラスターの構造および安定性が配位子 1 つに大きく依存することが明らかになった。

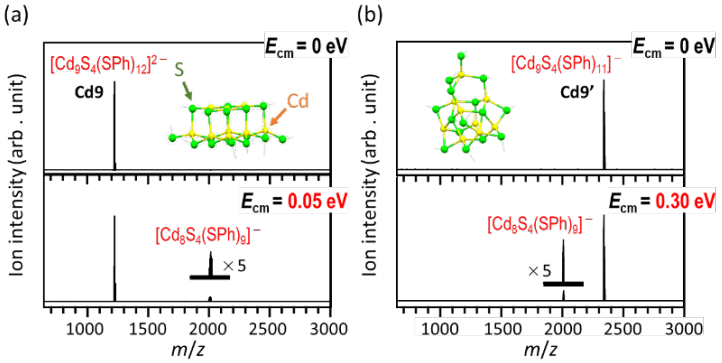

Fig. 1. CID mass spectra of (a) **Cd9** and (b) **Cd9'**. E_{cm} represents collision energy in the center-of-mass frame. Insets show DFT-optimized most stable structures while substituting the Ph groups to Me groups (wireframe).

(1) Muramatsu, S.; et al. *J. Phys. Chem. Lett.* **2023**, *14*, 5641. (2) Dance, I.; et al. *J. Chem. Soc., Chem. Commun*. **1982**, *21*, 1246.

日本化学会 第104春季年会 (2024)

イオン移動度質量分析によるフッ化銀クラスターカチオンの幾何構造の研究

（東北大理[1]・東北大院理[2]）○成瀬 優太[1]・坂倉 広也[2]・中島 優斗[2]・大下 慶次郎[2]・美齊津 文典[2]

Structures of silver fluoride cluster cations studied by ion mobility-mass spectrometry ([1]*Faculty of Science, Tohoku University*, [2]*Graduate School of Science, Tohoku University*) ○Yuta Naruse,[1] Hiroya Sakakura,[2] Yuto Nakajima,[2] Keijiro Ohshimo,[2] Fuminori Misaizu[2]

Neutral silver fluoride clusters Ag_nF_n (n = 2 - 5) have been reported to have stable planar ring structures, which are different from the bulk crystal structures [1], by quantum chemical calculations. In this study, geometrical structures of the silver fluoride cluster cations $Ag_nF_m^+$ were studied by ion mobility-mass spectrometry and quantum chemical calculations. The $Ag_nF_m^+$ clusters were generated by reacting laser-evaporated silver ions with a 2.5% SF_6/He gas mixture under the vacuum condition. 2D plots of m/z vs arrival time for $Ag_nF_m^+$ were obtained from the experiments (Fig. 1). The results of mass spectrometry indicated that $Ag_nF_{n-1}^+$, which has one less halogen atom than the metal atom ($m = n - 1$), was dominantly observed, as well as alkali halide clusters such as $Na_nF_m^+$ [2]. The collision cross sections were calculated from the arrival times, and the geometrical structures were assigned. Experimentally obtained collision cross sections indicate that the clusters $Ag_nF_m^+$ (n = 2 - 4) exhibit one- or two-dimensional structures, while a three-dimensional structural isomer emerges for n = 5.

Keywords: ion mobility-mass spectrometry; cluster; silver fluoride

フッ化銀中性クラスターAg_nF_nはn = 2 - 5 の組成において、バルク結晶とは異なる平面環状構造が安定であることが量子化学計算によって報告されている[1]。本研究では、イオン移動度質量分析と量子化学計算を用いて、クラスターカチオン$Ag_nF_m^+$の幾何構造を調べた。$Ag_nF_m^+$は真空中でレーザー蒸発させた Ag イオンと 2.5%SF_6/He 混合ガスとの反応により生成した。実験から質量電荷比ー到達時間 2 次元プロットが得られた（Fig. 1）。質量スペクトルには、$Na_nF_m^+$ [2]などのアルカリハライドクラスターと同様に、金属原子数に対してハロゲン原子数が 1 個不足した組成（$m = n - 1$）をもつ$Ag_nF_{n-1}^+$イオンが強く観測された。実験と計算結果との比較から、n = 2 - 4 の$Ag_nF_m^+$クラスターでは一次元・二次元構造を形成し、n = 5 ではこれらに加えて三次元構造の異性体も共存することが明らかになった。

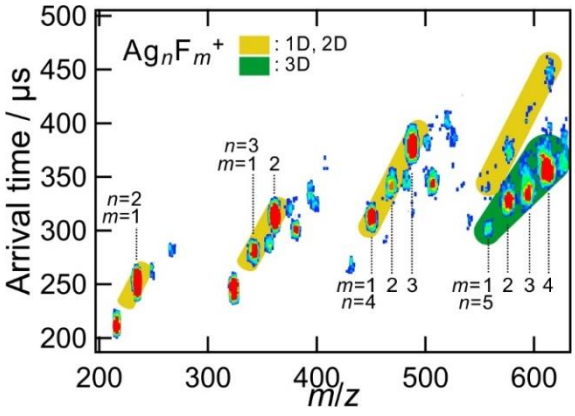

Fig. 1. 2D plot of m/z vs arrival time for $Ag_nF_m^+$.

[1] C.Song et al., *Comput. Theor. Chem.* **1074**, 157 (2015).

[2] K. Ohshimo et al., *J. Phys. Chem. A.* **118**, 9970-9975 (2014).

イオン画像観測法を用いた O_4^+ の紫外可視光解離過程に関する研究

（東北大理[1]・東北大院理[2]）○渡部 悠[1]・小柴 拓実[2]・伊藤 悠吏[2]・菅野 学[2]・大下 慶次郎[2]・美齊津 文典[2]

Ion imaging study on UV-Vis photodissociation processes of O_4^+

([1]*Faculty of Science, Tohoku Univ.*, [2]*Graduate School of Science, Tohoku Univ.*) ○Yu Watabe,[1] Takumi Koshiba,[2] Yuri Ito,[2] Manabu Kanno,[2] Keijiro Ohshimo,[2] Fuminori Misaizu[2]

O_4^+ clusters, known to be in the ionosphere of the Earth, have broad photodissociation cross sections in the UV-Vis range[1]. However, its photodissociation process is unclear. Therefore, we have performed ion imaging experiments for photofragment O_2^+ ions dissociated from O_4^+.

Mass-selected O_4^+ were irradiated with a linearly-polarized photolysis laser (355 nm), and the O_2^+ fragment ions were detected as a 2D image (**Fig. 1**). The image represented a highly positive anisotropy, which is consistent with the computational results demonstrating that the 4^2A_u excited state has a repulsive potential energy surface as indicated in **Fig. 2** and that the transition dipole moment $\boldsymbol{\mu}$ is parallel to the dissociation axis. Total kinetic energy release (TKER) derived from the obtained image was found to be a small fraction (less than 30 %) of the available energy (3.02 eV) as shown in **Fig. 1**. The large residual energy is partitioned into the electronic excitation, in addition to the rovibrational energies of the photofragments.

Keywords : Ion imaging; Photodissociation; Reaction dynamics; Molecular cluster; Atmospheric chemistry

酸素二量体クラスターカチオン O_4^+ は地球の電離層に存在し、紫外可視領域に幅広い光吸収断面積を持つことが知られている [1]。本研究では O_4^+ の光吸収反応のダイナミクスを調べるためにイオン画像観測実験を行った。

質量選別された O_4^+ に直線偏光の解離レーザー(355 nm)を照射して生じる解離生成物 O_2^+ の散乱分布画像を得た(**Fig. 1**)。得られた二次元画像は高い正の異方性を示した。これは紫外励起で生じる電子励起状態 4^2A_u が斥力的なポテンシャルをもつという励起状態計算の結果(**Fig. 2**)と対応している。また解離生成物の全並進エネルギー(TKER)は余剰エネルギー(3.02 eV)の 30 %以下にとどまり(**Fig. 1**)、多くのエネルギーは解離生成物の電子励起や振動回転エネルギーに分配されることが分かった。

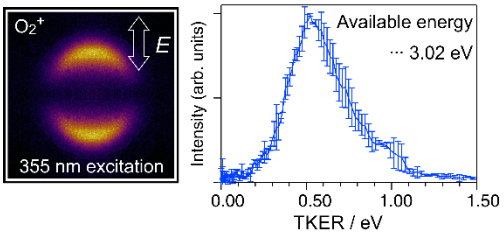

Fig. 1 An observed image (left panel) and a TKER distribution (right panel) of photofragments. (***E***: polarization direction of the photolysis laser)

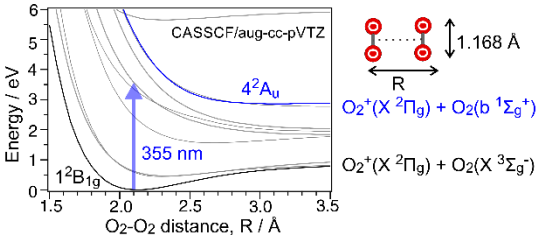

Fig. 2 Potential energy curves of the ground state (1^2B_{1g}) and the excited state (4^2A_u).

1) G. P. Smith *et al.*, *J. Chem. Phys.* **69**, 5393 (1978).

低温イオントラップ—イオン移動度質量分析を用いた分子内プロトン移動反応機構とその速度定数の研究

（東北大院理）○角田 健吾、布施 大輝、高崎 佑也、大下 慶次郎、美齊津 文典

Study of intramolecular proton transfer reaction mechanisms and their rate constants using cryogenic temperature ion trap-ion mobility mass spectrometry

(*Graduate School of Science, Tohoku University*)
○Kengo Tsunoda, Daiki Fuse, Yuya Takasaki, Keijiro Ohshimo, Fuminori Misaizu

Proton transfer reactions play an important role in chemical reactions in various environments. There are two isomers (protomers) in protonated *p*-aminobenzoic acid (PABA·H^+). We showed in a previous study using ion mobility-mass spectrometry that a single NH_3 molecule transports a proton between the two protonated sites in the reaction of PABA·H^+ with NH_3. In this study, the structure was determined for the reaction intermediates formed in a cooled ion trap. The proton transfer reaction rate constants were also determined. A correlation was found between the rate constants and the binding energies of ions with NH_3.

Keywords : Ion mobility-mass spectrometry; Proton transfer reaction; Vehicle mechanism; Grotthuss mechanism

プロトン付加 *p*-アミノ安息香酸（PABA·H^+）には、アミノ基の N 原子にプロトンが付加した N-プロトマー（**N-pr.**）と、カルボキシ基の O 原子にプロトンが付加した O-プロトマー（**O-pr.**）の 2 種の異性体が存在する。イオン移動度質量分析（IM-MS）では緩衝ガスとの相互作用の違いを利用してイオンを分離検出できる。以前に我々は IM-MS を用いて、PABA·H^+と NH_3 との衝突により NH_3 単分子がプロトンを運搬し **N-pr.**から **O-pr.**への異性化反応が起こることを示した[1]。本研究では反応場であるイオントラップを冷却し、その反応中間体（**PABA·H^+·NH_3**）の構造を同定した。結果としてイオントラップを 120 K まで冷却すると **PABA·H^+·NH_3** が観測され、イオンと緩衝ガスとの衝突断面積の比較から **O-pr.**への NH_3 付加物と同定された（**Fig. 1**）。この **PABA·H^+·NH_3** は理論計算からも最も安定な中間体であると帰属された。また 2 種類のイオンで反応速度定数を決定し、反応速度定数と NH_3 との結合エネルギーの間に相関があることを見出した。

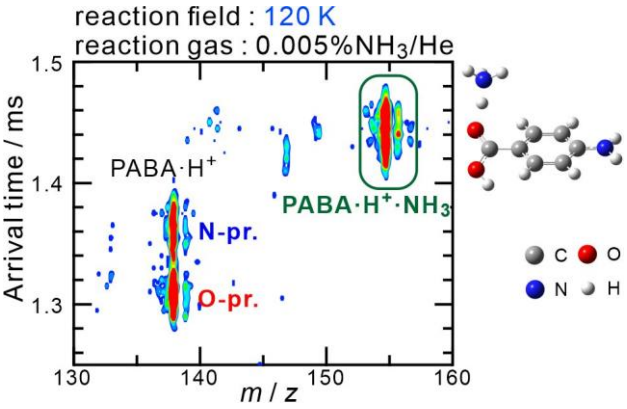

Fig. 1. 2D plots of arrival time vs mass number (*m*/*z*) for PABA·H^+. Structure of PABA·H^+·NH_3 is also shown.

[1] 大下、高崎、角田、伊藤、美齊津、日本化学会第 103 春季年会、野田、2023 年 3 月。

[2] K. Ohshimo, Y. Takasaki, K. Tsunoda, F. Misaizu et al., *J. Phys. Chem. Lett.* **14**, 8281 (2023).

低温イオン移動度質量分析によるメチルアンモニウムイオンージベンゾ-24-クラウン-8 錯体の異性体構造の研究

（東北大理 [1]・東北大院理 [2]）○渡辺喬介 [1]・伊藤亮佑 [2]・大下慶次郎 [2]・美齊津文典 [2]

Isomer structures of dibenzo-24-crown-8 complex with methylammonium ion studied by cryogenic ion mobility-mass spectrometry ([1]*Faculty and* [2]*Graduate School of Science, Tohoku Univ.*) ○Kyosuke Watanabe, [1] Ryosuke Ito, [2] Keijiro Ohshimo, [2] Fuminori Misaizu[2]

We performed cryogenic ion mobility-mass spectrometry of the methylammonium ion - dibenzo-24-crown-8 [$CH_3NH_3^+$(DB24C8)] complex. A bimodal feature was obtained for the ion arrival time distribution. The components with short and long arrival times were assigned to the conformers in which the methyl groups of $CH_3NH_3^+$ were oriented in the same and opposite directions as the two benzene rings, respectively. We thus concluded that the direction of the guest ion determines the two conformations of the complex with different cross sections.
Keywords : Structural isomer; Host-guest compounds; Ion mobility-mass spectrometry; Crown ether

クラウンエーテルは、ホスト分子としての選択性やその構造変換の容易さから、アルカリ金属イオンを始めとした様々な無機イオンのセンサーに用いられている。ジベンゾ-24-クラウン-8（DB24C8, Fig. 1a）は NH_4^+とも錯形成し、NH_4^+(DB24C8)の低温イオン移動度質量分析（IM-MS）により、二つのベンゼン環の間の距離が異なる 2 種類のコンフォマー（closed, open）が共存することが知られている [1)]。本研究では $CH_3NH_3^+$(DB24C8)の異性体を低温 IM-MS で分離し、その構造を同定した。

到達時間分布は NH_4^+(DB24C8)と同様に 2 成分に分かれ、到達時間が遅い成分は NH_4^+(DB24C8)と同様の open 構造（Fig. 1b）に帰属した。一方、速い成分の衝突断面積（CCS）は closed 構造（Fig. 1c）に加えて、NH_4^+(DB24C8)とは異なる最安定構造（Fig. 1d）の CCS の計算値とも一致した。Open 構造では $CH_3NH_3^+$のメチル基が二つのベンゼン環の側を向いているが、closed 構造と最安定構造ではメチル基が二つのベンゼン環とは反対側を向いていることが分かった。したがって、ゲストイオンが配位する方向によって、錯体の立体構造が変わると結論した。

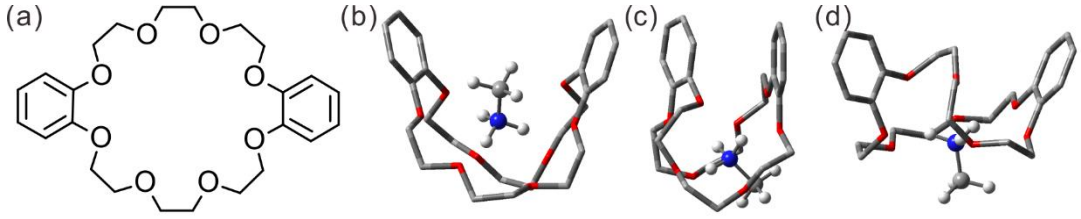

Fig. 1. (a) Structural formula of DB24C8, stable structures of (b) open and (c) closed conformers, and (d) the most stable structure of $CH_3NH_3^+$(DB24C8) optimized at M06-2X/6-311++G(d,p) level.

1) R. Ito, K. Ohshimo, and F. Misaizu, *Chem. Phys. Lett.* **794**, 139510 (2022).

Control of charge state and reactivity of single-sized silver nanoclusters supported on organic substrates

([1]*Keio University*) ○Takashi Nishikawa[1], Koh Shinomiya[1], Tomoya Inoue[1], Atsushi Nakajima[1]
Keywords: Nanocluster; Silver; Oxidative reactivity; X-ray photoelectron spectroscopy;

Silver (Ag) is widely used in industrially essential catalytic reactions, such as Ullmann-type coupling reactions. Nanoclusters (NCs), composed of dozens of atoms, can design a variety of electronic states and high reactivity by atomically defining their size and by controlling their charge states. Developing NC-based catalysts requires a chemically stable surface support that prevents poisoning and degradation caused by reactions with unwanted gas molecules. An example of poisoning is the reaction with molecular oxygen (O_2), the most common active gas in the atmosphere. In this study, single-sized Ag_{21} NCs were deposited on *p*-type hexa-*tert*-butyl-hexa-*peri*-hexabenzocoronene ($C_{66}H_{66}$: HB-HBC) modified substrates[1], and their charge states and reactivity at room temperature with O_2 were measured by ultraviolet/X-ray photoelectron spectroscopy (UPS/XPS).

Cationic Ag NCs synthesized in the gas phase by magnetron sputtering were size-selected using a quadrupole mass spectrometer and deposited under soft landing conditions. 0.6 monolayer (ML) of Ag_{21}^+ was deposited on graphite substrates modified with a 2 nm thick HB-HBC layer. The samples were transported to a photoelectron spectrometer while maintaining ultra-high vacuum (~10^{-8} Pa) to investigate the charge and chemical state of the NCs by UPS/XPS measurements (He I α: $h\nu$ = 21.22 eV, Mg Kα: $h\nu$ = 1253.6 eV). The sample was exposed to O_2 molecules defined in Langmuir (10^{-6} Torr・s) units at room temperature, and the reactivity of the surface-supported Ag_{21} was evaluated using XPS measurements. Figure 1(a) shows the UPS spectra before and after Ag_{21} deposition on the HB-HBC substrate. The peak position of the HOMO−2 of Ag_{21}/ HB-HBC is about 0.7 eV larger than the 3.31 eV of the HB-HBC$^+$ substrate (green line) where the HB-HBC is +1-valent. This suggests that the Ag_{21} deposited HB-HBC substrate is strongly positively charged, while the Ag_{21} takes on a large negative charge, forming a multivalent charge transfer state in Ag_{21}/ HB-HBC. Figure 1(b) shows the XPS spectra around O 1*s* core levels before and after exposing 10^{14} L of O_2 to Ag_{21}/HB-HBC. There is almost no difference in intensity before and after exposure. Therefore, by using an HB-HBC modified substrate, we achieved a surface-supporting method that controls the charge state and suppresses poisoning by O_2. These results are promising for the development of nanocatalysts based on nanoclusters that can be used under atmospheric pressure.

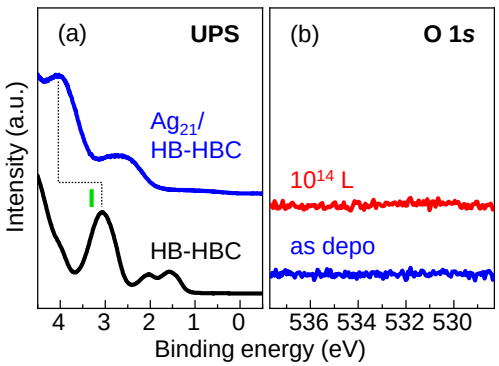

Fig. 1. (a) UPS spectra for an HB-HBC substrate before and after 0.6 ML of Ag_{21} deposition. (b) XPS spectra of O 1*s* core levels for Ag_{21}/HB-HBC (0.6 ML) before and after 10^{14} L of O_2 exposure.

1) *J. Phys. Chem. C* **2022**, 126, *26*, 10889−10899

時間波形測定による四塩化炭素液滴中の高次誘導ラマン散乱発生機構の解明

（学習院大理）○片岡　留伊慈・河野　淳也

Generation of multiorder stimulated Raman scattering in CCl_4 droplets studied by temporal profiles (*Department of Chemistry, Faculty of Science, Gakushuin University*)

○Ruiji Kataoka, Jun-ya Kohno

A droplet acts as an optical cavity. When a droplet is irradiated with a laser, Raman scattered light gains its intensity by resonance at the droplet surface. In this study, we measured temporal waveforms of multiorder stimulated Raman scattered light (SRS) generated by laser irradiation to a single droplet and colliding droplets of CCl_4. Obtained Raman spectra consist of many peaks assignable to the multiorder SRS of CCl_4. Here, we focus on the multiorder SRS bands of the symmetric stretching vibrational mode of CCl_4. The temporal waveforms of the SRS were measured for each laser pulse simultaneously with the spectrum or the image.

Figure 1a shows a typical temporal waveform of the first order SRS. The temporal waveform consists of two peaks, which are fitted by Gaussian functions. Figure 1b shows the generation times of the two peaks are function of the number of the SRS order. The generation time decreases as the number of the order increases. This result indicates that the lower the order number is, the longer the SRS light resonates in the droplet before the emission from the droplet. In the presentation, we discuss the origin of the two peaks in the temporal waveforms.

Keywords : microdroplets; multiorder stimulated Raman scattering, cavity enhancement

液滴は光共振器として働く。液滴にレーザーを照射すると、ラマン散乱光は液滴表面で共振し、誘導ラマン散乱光(SRS)として増強する。また、SRS を光源とする高次 SRS の発生も見られる。本研究では、その増強機構を明らかにするため、四塩化炭素の微小液滴へのレーザー照射により発生する高次 SRS の発生時間の測定を行った。四塩化炭素には四つの振動モードがあり、それらの重ね合わせによって多くのラマンスペクトルのピークが観測される。その中でも、全対称伸縮振動に注目して実験を行った。ピエゾ素子駆動のノズルによって生成された微小液滴に Nd:YAG レーザーの第二高調波である 532 nm の光を照射した。発生したラマン散乱光を 7:3 のビームスプリッターで分離し、3 割の光で画像を観測した。残った 7 割の光はハーフミラーでさらに二つに分離し、それぞれ時間波形とラマンスペクトルの測定に用いた。時間波形は画像またはスペクトルと同時にレーザーパルス毎に測定した。

測定した時間波形(Fig.1a)には二つのピークがあった。この二つのピークのガウス関数フィッティングにより高次 SRS の発生時間を求めた。得られた発生時間の次数依存性を Fig.1b に示す。ここから、次数が大きくなるにつれて発生時間が短くなっていることが分かった。これは、低次光が高次光に比べて長く液滴内で共振していて、液滴から光が出るまで時間がかかるからであると考えられる。発表では二つのピークの生成機構を含めて詳細に議論する。

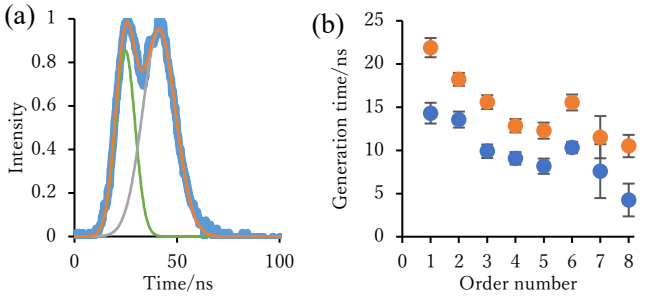

Fig. 1　(a) Temporal waveform of the first order SRS. (b) The generation times of the multiorder SRS as a function of the order number.

液滴分子線赤外レーザー蒸発法とデジタルイオントラップを用いた気相イオン蛍光分光装置の開発

（学習院大理）○奥津 賢一・岡 巧・水村 華子・河野 淳也
Development of gas-phase ion fluorescence spectrometer combined with digital ion trap using droplet-beam IR laser ablation method (*Faculty of Science, Gakushuin University*) ○Kenichi Okutsu, Takumi Oka, Hanako Mizumura, and Jun-ya Kohno

We have been using the Droplet-Beam Laser Ablation Mass Spectrometry (DB-LAMS) method to investigate the structure and properties of biomolecules. This technique allows us to observe biomolecules in a state close to the solution phase, as it generates ions with lower charge states compared to the electrospray ionization method. Previously, we have developed and reported a gas-phase resonance Raman / fluorescence spectroscopy apparatus combined with this method. Also, we have developed a new method to extract the fluorescence out of the vacuum chamber directly to a spectrometer in the atmosphere, aiming for more efficient observations. Additionally, in order to improve the mass resolution, we are planning to introduce square wave voltage, also known as digital ion trap[1)], in combination with “plate” electrodes. By using the plate shape electrode, it will be able to achieve ideal electrostatic field for ion acceleration. We will report the results of the mass spectrum of trapped Rhodamine 6G (Rh6G) ions and the fluorescence extraction examined by using Rh6G aqueous droplets.
Keywords : Fluorescence spectroscopy; Apparatus development; Droplet; Digital ion trap; Mass spectrometry

我々のグループでは液滴分子線赤外レーザー蒸発(DB-LAMS)法を用いて気相生体分子の構造や物性などを調べてきた。この手法ではイオン化においてエレクトロスプレーイオン化法と比べ価数の低いイオンが生成し、生体分子を溶液中に近い状態で観測できる。これまでに DB-LAMS 法と組み合わせた気相蛍光/共鳴ラマン分光装置を開発し報告した。一方、気相単離されたイオンの蛍光分光において、例えばその溶媒和などを調べるためには高い質量分解能が求められる。そこで我々はイオントラップに矩形波電圧を適用するデジタルイオントラップ(DIT)[1)]を電極「板」の導入と合わせて進めている。DIT の導入により周波数の変更が容易になり、また電極板の導入によりイオン加速に適した電場勾配を作り出すことが期待できる。本発表ではトラップしたローダミン 6G イオンの質量スペクトルおよび蛍光取り出し結果について報告する。

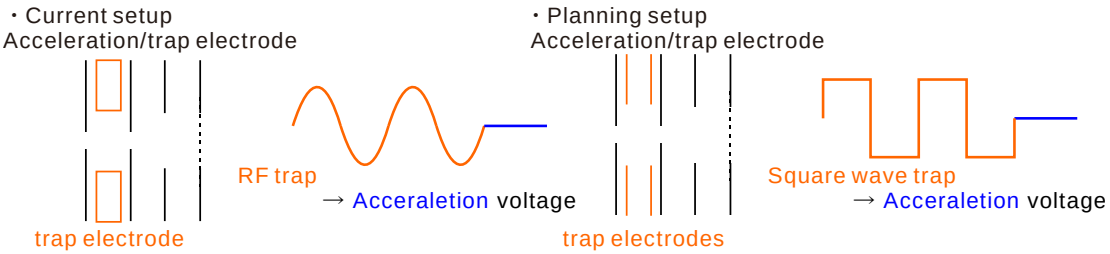

1) A digital ion trap mass spectrometer coupled with atmospheric pressure ion sources. L. Ding, M. Sudakov, et al. *J. Mass Spectrom.* **2004**, *39*, 471-484.

Dependence of the oscillation of N_2^+ lasing signals at 391 nm on the wavelength of seed laser pulses

([1] *School of Science, University of Tokyo*, [2]*NTT Advanced Technology Corporation*)
○Tomoya Yamauchi,[1] Hiroki Mashiko,[2] Toshiaki Ando,[1] Erik Loetstedt,[1] Atsushi Iwasaki,[1] Kaoru Yamanouchi[1]
Keywords: air lasing; N_2^+; strong field ionization; population transfer; intense field science

When an intense femtosecond near-infrared laser (NIR) pulse is focused into air, a coherent light at 391 nm is emitted from the ionized nitrogen molecules via the $B^2\Sigma_g^+$–$X^2\Sigma_u^+$ (0,0) transition. This phenomenon is called "air lasing",[1] and one mechanism proposed to explain this is the superradiance-type emission[2]. By NIR-UV pump-probe experiments, the time dependent amplification of the air lasing signal has been investigated[3]. Among the observed oscillations, those appearing when the pump and probe pulses overlap temporally have not been investigated thoroughly. Here we examine the origin of the characteristic oscillations by NIR-UV pump-probe measurements in which the spectrum of the probe pulses is varied systematically using a 4-*f* system. In the 4-*f* system, the shorter wavelength side of the spectrum of the seed pulse was cut off by the movable beam block placed at the Fourier plane.

Figure 1 shows the observed lasing intensity as a function of the pump-probe time delay. As can be seen in (b) and (c) in Fig. 1, when the components resonant to the B–X transition are cut off, the amplification occurs only when the pump and probe pulses temporally overlap. In addition, as can be seen in (a) and (b) in Fig. 1, a fast oscillation appears in this delay time region, whose period becomes longer when the spectrum of the probe pulse becomes narrower. This oscillation can be attributed to the interference between the phase in the coherence induced by the off-resonant components and that induced by the resonant 391 nm components. Even when only the off-resonant components are included, the coherence increases during the temporal overlap between the pump and probe pulses. The increase in the coherence is considered to be caused by the AC Stark shift induced by the pump pulse.

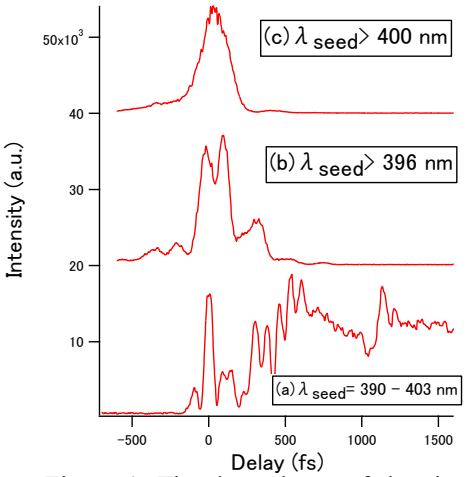

Figure 1. The dependence of the signal intensity of N_2^+ lasing at 391.8 nm on the pump-probe delay time. The spectral ranges of the seed pulses are (a) λ_{seed} = 390–403 nm, (b) λ_{seed} > 396 nm, and (c) λ_{seed} > 400 nm.

1) L. Yuan, et al., *Adv. Quantum Technol.* **2019**, *2*, 1900080. 2) H. Chao, et al., *Opt. Lett.*, **48**, 526 (2023). 3) M. Britton, et al., *Phys. Rev. A*, **100**, 013406 (2019).

Reactions of Iron Cationic Clusters with Hydrogen Molecules Investigated by Gas-phase Thermal Desorption Spectrometry

(*Graduate School of Arts and Science, The University of Tokyo*) ○ Xueshan Wu, Yufei Zhang, Masato Yamaguchi, Toshiaki Nagata, Ken Miyajima, Fumitaka Mafuné

Keywords: Gas-phase Cluster, Temperature Programmed Desorption, Iron Hydride, Mass Spectrometry

The interaction of hydrogen with transition metals plays a significant role in the field of hydrogen storage, among which iron has attracted considerable attention as one of the most common elements on Earth.[1,2] Previous studies have revealed that Fe cluster cations show a large size effect against H_2.[1,3] This study investigated the desorption of H_2 using gas-phase thermal desorption spectrometry (TDS).

$Fe_nH_m^+$ clusters were prepared by laser ablation of an iron rod with 1% H_2 seeded He carrier gas and then were heated from 330 K to 1000 K. At 330 K, the fraction of hydrogenated clusters ($m \geq 1$) for small Fe clusters (n = 4–6) was higher than that for larger clusters (n = 7–12). During the heating process, sequential desorption of H_2 was observed.

Fig. 1 shows the average number of H atoms (m_{ave}) and m_{ave} per Fe atom (m_{ave}/n; atomic ratio) in $Fe_nH_m^+$ clusters. The m_{ave} slightly decreased for $Fe_{4–9}H_m^+$ in the low-temperature range (<550 K), whereas for large clusters ($Fe_{10–12}H_m^+$), it stayed almost constant. Hydrogen desorption from the clusters was observed at 550–750 K, and most desorption was completed at 800 K. $Fe_4H_m^+$ clusters continuously released hydrogen up to 1000 K, demonstrating exceptional thermal durability. For large clusters ($n \geq 8$), m_{ave}/n increased with an increase in the size of the clusters (Fig. 1b).

It is worth mentioning that not only n = 4 but also n = 5 has a significantly high m_{ave}/n of approximately 0.97 at 330 K, indicating large H atom uptake.

Among the Fe_n^+ clusters, $Fe_{4,5}^+$ exhibited unique desorption features for both large H atom uptake and thermal durability. To further investigate the results, the details of the structures and desorption energies of the $Fe_{4,5}H_m^+$ clusters are discussed.

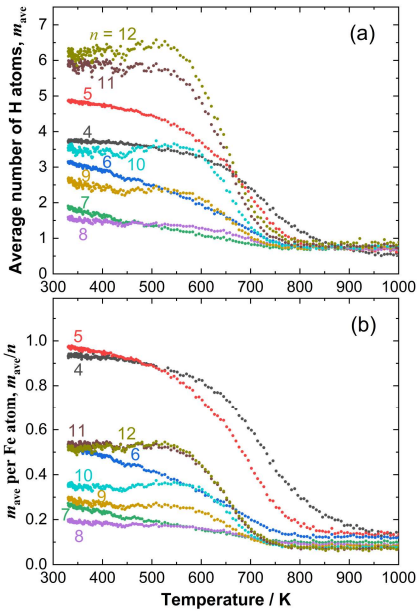

Fig. 1. Temperature dependence of (a) average number of H atoms in $Fe_nH_m^+$ clusters, m_{ave}, and (b) average number of H atoms per Fe atom, m_{ave}/n.

1) I. Swart, F. M. F. de Groot, B. M. Weckhuysen, P. Gruene, G. Meijer, and A. Fielicke, *J. Phys. Chem. A* **2008**, 112, 1139. 2) T. J. Dhilip Kumar, P. Tarakeshwar, and N. Balakrishnan, *Phys. Rev. B* **2009**, 79, 205415. 3) R. L. Whetten, D. M. Cox, D. J. Trevor, and A. Kaldor, *Phys. Rev. Lett.* **1985**, 54, 1494.

気相昇温脱離法を用いたロジウムクラスターの水素吸蔵性能の研究

（東大・総合文化）○藏下 隼人・呉 楊琨・工藤 聡・山口 雅人・永田 利明・宮島 謙・真船 文隆

Hydrogen Storage Capacity of Rhodium Clusters Studied by Thermal Desorption Spectrometry in the Gas Phase (*Graduate School of Arts and Sciences, The University of Tokyo*)○Hayato Kurashita, Yangkun Wu, Satoshi Kudoh, Masato Yamaguchi, Toshiaki Nagata, Ken Miyajima, Fumitaka Mafuné

Gas-phase Rh clusters as well as Pd and V clusters are known to adsorb and release hydrogen, and have been studied in the context of hydrogen storage alloys. In this study, hydrogenated rhodium clusters, $Rh_nH_m^+$, were prepared by the laser ablation method in the presence of H_2. The temperature dependence of their compositions was investigated by the gas-phase thermal desorption spectrometry to elucidate the hydrogen storage capability.

$Rh_nH_m^+$ clusters possessed 2–5 times as many H atoms as Rh atoms ($m/n \approx 2$–5) at 300 K. More than half of the H atoms desorbed at 500 K. Rh clusters were found to adsorb more hydrogen atoms at 300 K and desorbed hydrogen molecules at lower temperatures than Pd, V, and Al-Nb clusters.

Keywords : Rhodium; Cluster; Hydrogen; Thermal Desorption Method

パラジウムなどの金属は水素吸蔵能力があることが知られている。水素吸蔵の詳細な機構を知るため各金属の気相クラスターを用いた研究が行われており、パラジウム、バナジウムなどと同様にロジウムのクラスターの水素吸着が報告されている [1–4]。本研究では気相中で $Rh_nH_m^+$を生成し、気相昇温脱離法により各温度での組成を調べ、Pd, V , Al–Nb 合金クラスターの結果と比較し、水素との親和性の違いを検討した。

$Rh_nH_m^+$ (n = 2–7)は 300 K において、各サイズとも Rh 原子数の 2–5 倍程度の H 原子を吸着し($m/n \approx 2$–5)、500 K までの加熱で過半数の水素原子が脱離した(Fig. 1)。Fig. 2 は $Rh_4H_m^+$, $Pd_4D_m^+$, $V_4H_m^+$, $Al_4NbH_m^+$について H/D 原子数の加重平均を温度ごとにプロットしたものである。室温で $Rh_4H_m^+$の m の加重平均は 15 を超えていたのに対し、$Pd_4D_m^+$は 4 に満たなかった。また 350–600 K の間に $Rh_4H_m^+$は H 分子を多く脱離する一方、$Pd_4D_m^+$, $Al_4NbH_m^+$, $V_4H_m^+$はあまり H/D を脱離しなかった。$Rh_4H_m^+$クラスターで観測された H の最大吸着数が多く、加熱により速やかに脱離する傾向は n = 4 以外のサイズでも見られた。このことから Rh は水素吸蔵合金の特性を向上させることが期待される。

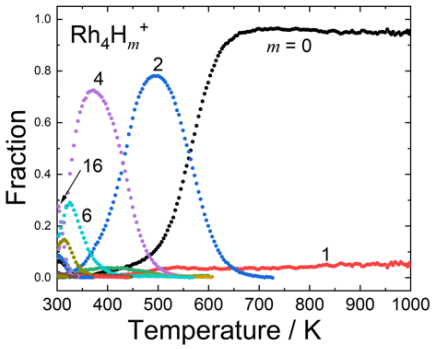

Fig. 1 Fraction of $Rh_4H_m^+$ as a function of the temperature.

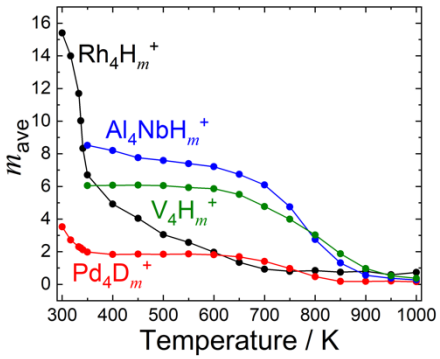

Fig. 2 Average m (m_{ave}) of $Rh_4H_m^+$, $Pd_4D_m^+$, $Al_4NbH_m^+$, and $V_4H_m^+$.

1) M. Takenouchi, S. Kudoh, K. Miyajima, F. Mafuné, *J. Phys. Chem. A* **2015**, 119, 6766–6772.
2) Y. Zhang, F. Mafuné, *J. Phys. Chem. Lett.* **2023**, 14, 5734–5739.
3) Y. Wu, K. Miyajima, S. Kudoh, T. Nagata, F. Mafuné, *J. Phys. Chem. A* **2023**, 127, 8821–8827.
4) P. Ferrari, H. T. Pham, J. Vanbuel, M. T. Nguyen, A. Fielicke, E. Janssens, *Chem. Commun.*, **2021**, 57, 9518-9521

Computational Investigation on Hydrogen Storage Capacity of Transition Metal Dimers

(*Graduate School of Arts and Sciences, The University of Tokyo*)
○Yufei Zhang, Masato Yamaguchi, Toshiaki Nagata, Satoshi Kudoh, Ken Miyajima, Fumitaka Mafuné

Keywords: Gas phase clusters; Hydrogen storage; Transition metal; DFT calculation

Hydrogen is known as a promising alternative energy carrier which has advantages such as clean combustion and light weight compared with carbon-based fossil fuel.[1] Appropriate storage material for hydrogen is necessary to achieve practical application. Hydrides of light metals such as Al are one of the ideal storage materials. However, Al hydrides cannot be formed under practical conditions. Previous researches suggested that doping of transition metal (TM) can tune the hydrogen dissociation from bulk-phase materials to the cluster level.[2,3] Therefore, understanding of interaction between TM atoms and hydrogen becomes important. In this study, hydrogen adsorption on TM (Co, Rh, Ir, and Cu) dimers was investigated by gas-phase experiments and DFT calculations.

TM dimers were prepared by laser ablation of a TM rod in a H_2 seeded He carrier gas. Fig. 1a shows the fractional distribution of $Co_2H_i^+$, $Rh_2H_i^+$,[4] $Ir_2H_i^+$, and $Cu_2H_i^+$ in gas phase experiments. Co_2^+ and Cu_2^+ show less reactivity against hydrogen. Fig. 1b presents the binding energies of H_2 molecules on $M_2H_{2(p-1)}^+$ obtained by DFT calculations. Co_2^+ and Cu_2^+ have smaller binding energies than these of Rh_2^+ and Ir_2^+ while the first H_2 adsorbs molecularly, suggesting that H_2 adsorption and desorption reach the equilibrium. As the result, further H_2 adsorption on Co_2^+ and Cu_2^+ was hindered. The details of hydrogen adsorption forms on those dimers as well as their electronic structures will be discussed.

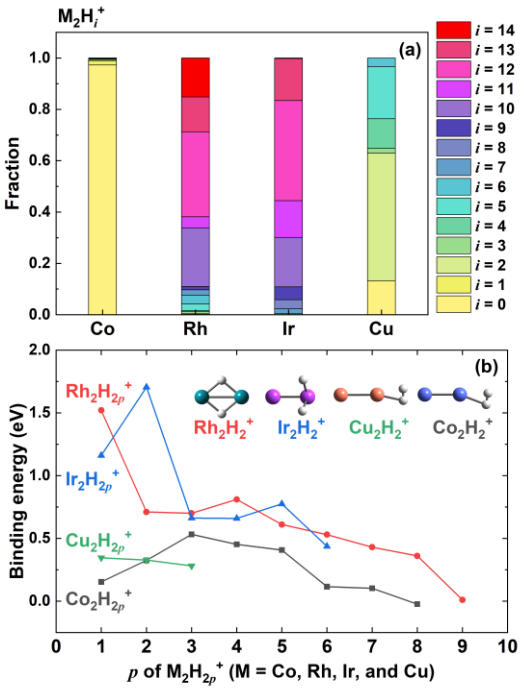

Figure 1 (a) Fractional distribution of $M_2H_i^+$ at room temperature. (b) Binding energies of H_2 on $M_2H_{2(p-1)}^+$ and geometries of $M_2H_2^+$; M = Co (blue), Rh (cyan), Ir (purple), and Cu (pink).

1) J. Graetz, *Chem. Soc. Rev.* **2009**, 38, 73–82.
2) S. Chaudhuri, *et. al.*, *J. Am. Chem. Soc.* **2006**, 128, 11404–11415.
3) Y. Zhang, *et. al.*, *J. Phys. Chem. Lett.* **2023**, 14, 25, 5734–5739.
4) H. Kurashita, *et. al.*, The 17th Annual Meeting of Japan Society for Molecular Science, **2023**, 4P064.

熱的条件下における貴金属クラスターの光電子イメージング

(東大院総合) ○山口 雅人，立川 慧太郎，永田利明，宮島 謙，真船 文隆
Photoelectron Spectroscopy of Precious Metal Clusters under Heating Conditions
(The University of Tokyo) ○Masato Yamaguchi, Keitaro Tatsukawa, Toshiaki Nagata, Ken Miyajima, Fumitaka Mafuné

The adsorption forms of reactants on catalysts are important for their reactivity. In this study, we focused on how the electronic/geometric structures were changed after the clusters underwent heating. The Rh_3NO^- clusters were generated by laser ablation of a Rh rod in the presence of a He/NO mixture in the gas phase. The clusters were heated and then spatially separated by TOF-MS before being irradiated with a laser (355 nm, 3.55 eV) to obtain photoelectron images using velocity map imaging (VMI). The heating of the Rh_3NO^- clusters induced some changes in the photoelectron spectrum; a peak around 2.1 eV in binding energy decayed gradually with increasing temperature up to 500 K.

Keywords：Gas-Phase Cluster, Photoelectron Spectroscopy, Precious Metal

本研究では小分子の吸着したクラスターが熱的条件下でどのような電子・幾何構造変化を起こすのかに着目した．NO/He 混合気体存在下で Rh 金属試料をレーザー蒸発することで Rh_nNO^-を生成した．生成したクラスターは温度制御した加熱管を通過した後，TOF-MS によって空間的に分離された．目的のクラスターに対し，光電子脱離用レーザー(355 nm, 3.55 eV)を照射し，velocity map imaging (VMI)により光電子スペクトルを取得した．Rh_3NO^-は加熱することで特定の結合エネルギーのピークが消滅する[1–2]. 50 K 刻みで室温から 800 K まで温度を変更しながら光電子スペクトルを取得し比較を行った．その結果，2.1 eV 付近に観測されたピークは室温から加熱すると徐々に強度が減少しほぼ 500 K で消失した(Figure 1)．一方，>2.3 eV のピークは加熱によって線幅が広がるなどの形状変化は見られるものの，他のピークとの相対強度が大きく変わることはなかった．これらの観測結果を時間依存密度汎関数法(TD-DFT)による量子化学計算と合わせて議論する．

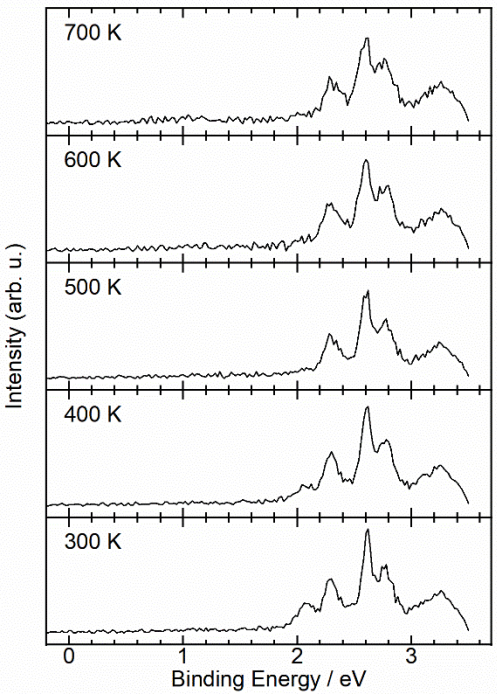

Figure 1. Temperature dependence of photoelectron spectra of Rh_3NO^-.

[1] 山口 雅人，日本化学会 第 102 春季年会, F102-1am-08 (2022)
[2] 立川 慧太郎，第 16 回分子科学会, 1B01 (2022)